

The Ghd7 transcription factor represses *ARE1* expression to enhance nitrogen utilization and grain yield in rice

Qing Wang^{1,2,3,8}, Qingmei Su^{3,4,8}, Jinqiang Nian^{1,3,8}, Jian Zhang¹, Meng Guo^{1,8}, Guojun Dong⁵, Jiang Hu⁵, Rongsheng Wang^{1,3}, Changshuo Wei^{1,3,8}, Guanwen Li⁶, Wan Wang^{1,8}, Hui-Shan Guo^{2,3}, Shaoyang Lin^{1,3,8}, Wenfeng Qian^{1,3,8}, Xianzhi Xie⁷, Qian Qian⁵, Fan Chen^{3,4,8,10,*} and Jianru Zuo^{1,3,8,9,10,*}

¹State Key Laboratory of Plant Genomics, Institute of Genetics and Developmental Biology, Chinese Academy of Sciences, Beijing 100101, China

²State Key Laboratory of Plant Genomics, Institute of Microbiology, Chinese Academy of Sciences, Beijing 100101, China

³University of Chinese Academy of Sciences, Beijing 100049, China

⁴State Key Laboratory of Molecular Developmental Biology, Institute of Genetics and Developmental Biology, Chinese Academy of Sciences, Beijing 100101, China

⁵State Key Laboratory of Rice Biology, China National Rice Research Institute, Hangzhou 310006, China

⁶Chinese Research Academy of Environmental Sciences, Beijing 100012, China

⁷Shandong Rice Research Institute, Shandong Academy of Agricultural Sciences, Jinan 250100, China

⁸Innovation Academy for Seed Design, Chinese Academy of Sciences, Beijing 100101, China

⁹CAS Center for Excellence in Molecular Plant Sciences, Chinese Academy of Sciences, Beijing 100101, China

¹⁰Hainan Yazhou Bay Seed Laboratory, Sanya 572025, China

*Correspondence: Fan Chen (fchen@genetics.ac.cn), Jianru Zuo (jrzuo@genetics.ac.cn)

<https://doi.org/10.1016/j.molp.2021.04.012>

ABSTRACT

The genetic improvement of nitrogen use efficiency (NUE) of crops is vital for grain productivity and sustainable agriculture. However, the regulatory mechanism of NUE remains largely elusive. Here, we report that the rice *Grain number, plant height, and heading date7* (*Ghd7*) gene genetically acts upstream of *ABC1 REPRESSOR1* (*ARE1*), a negative regulator of NUE, to positively regulate nitrogen utilization. As a transcriptional repressor, *Ghd7* directly binds to two Evening Element-like motifs in the promoter and intron 1 of *ARE1*, likely in a cooperative manner, to repress its expression. *Ghd7* and *ARE1* display diurnal expression patterns in an inverse oscillation manner, mirroring a regulatory scheme based on these two loci. Analysis of a panel of 2656 rice varieties suggests that the elite alleles of *Ghd7* and *ARE1* have undergone diversifying selection during breeding. Moreover, the allelic distribution of *Ghd7* and *ARE1* is associated with the soil nitrogen deposition rate in East Asia and South Asia. Remarkably, the combination of the *Ghd7* and *ARE1* elite alleles substantially improves NUE and yield performance under nitrogen-limiting conditions. Collectively, these results define a *Ghd7-ARE1*-based regulatory mechanism of nitrogen utilization, providing useful targets for genetic improvement of rice NUE.

Key words: nitrogen utilization, rice, *Ghd7-ARE1*, transcriptional repression, molecular breeding

Wang Q., Su Q., Nian J., Zhang J., Guo M., Dong G., Hu J., Wang R., Wei C., Li G., Wang W., Guo H.-S., Lin S., Qian W., Xie X., Qian Q., Chen F., and Zuo J. (2021). The Ghd7 transcription factor represses *ARE1* expression to enhance nitrogen utilization and grain yield in rice. *Mol. Plant*. **14**, 1–12.

INTRODUCTION

Nitrogen is an essential element for all living organisms, and plants are the primary source of the nitrogen cycle in the ecosystem. In plants, nitrogen utilization involves multiple tightly coupled processes, mainly including uptake, transport, assimilation, and remobilization or reutilization. Inorganic nitrogen absorbed from the soil, mainly in the form of nitrate and ammo-

nium, is assimilated into amino acids, mediated mainly by the glutamine synthetase/glutamine:2-oxoglutarate aminotransferase (GS/GOGAT) cycle (Xu et al., 2012; Krapp, 2015). Null mutations in the barley *GS2* and the rice ferredoxin-dependent

Molecular Plant

GOGAT (*Fd-GOGAT*; also known as *ABNORMAL CYTOKININ RESPONSE1* or *ABC1*) genes cause a seedling-lethal phenotype (Wallsgrrove et al., 1987; Yang et al., 2016).

In rice, nitrogen positively regulates various important agronomic traits, including plant height, tiller number, chlorophyll content, heading date, grain number, and, eventually, grain yield (Singh et al., 2014; Wang et al., 2014; Ye et al., 2019). Extensive efforts have been made in attempts to increase nitrogen use efficiency (NUE), targeting various components of nitrogen metabolism and potential regulators of NUE (Good et al., 2004; McAllister et al., 2012). Allelic variants in genes for nitrate transporters, nitrate reductase, and an unknown-function protein *ARE1* (for *abc1 REPRESSOR1*) display distinctive divergence among varieties, of which those in the *indica* or wild rice variants are proposed to contribute a higher NUE (Hu et al., 2015; Wang et al., 2018a; Gao et al., 2019; Tang et al., 2019). Several transcription factors, including GRF4, NGR5, and Nhd1, have been shown to be key regulators of NUE by modulating gibberellin and light signaling (Li et al., 2018; Wu et al., 2020; Zhang et al., 2021). Notably, *Grain number, plant height, and heading date7* (*Ghd7*), also encoding a transcription factor, modulates multiple agronomic traits regulated by nitrogen (Xue et al., 2008; Weng et al., 2014). At least 10 natural allelic variants of *Ghd7* have been identified (Xue et al., 2008; Lu et al., 2012; Saito et al., 2019). Of those variants, the fully functional alleles *Ghd7-1* and *Ghd7-3* are found in varieties grown in areas with hot summers and long growing seasons, whereas the *Ghd7-2* weak allele is found mainly in temperate *japonica* varieties. The nonfunctional null alleles *Ghd7-0* and *Ghd7-0a* are present in varieties with short growing seasons (Xue et al., 2008). Thus, the heading date is likely a major trait in the selection of *Ghd7* during breeding, targeting both the productivity and the environmental adaptability.

The *ARE1* gene encodes a plastid-localized protein with unknown function (Wang et al., 2018a). Multiple allelic variants of *ARE1* have also been identified. Among these natural alleles, three major variants, *ARE1^{NPB}*, *ARE1⁹³¹¹*, and *ARE1^{MH63}*, have been characterized, which are predominantly present in *japonica* and *indica* varieties, respectively. The *ARE1⁹³¹¹* and *ARE1^{MH63}* variants carry small insertions of 6 bp at different positions in the *ARE1* promoter, causing a reduction in the *ARE1* transcription that is negatively correlated to grain yield (Wang et al., 2018a). In this study, we show that *Ghd7* directly binds to two Evening Element-like (EEL) motifs in *ARE1* to repress its expression, thereby positively regulating nitrogen utilization. Moreover, the elite alleles of *Ghd7* and *ARE1* might have been subjected to diversifying selection during breeding and their allelic distribution is associated with the soil nitrogen deposition rate (NDR). We also demonstrate that the combination of elite alleles of *Ghd7* and *ARE1* increases NUE and grain yield under low-nitrogen conditions, thus providing a new strategy for crop NUE improvement.

RESULTS AND DISCUSSION

Ghd7 acts genetically upstream of *ARE1* to modulate nitrogen utilization

To assess potential genetic interactions between *Ghd7* and *ARE1*, we generated a series of near-isogenic line (NIL) plants with various combinations of *Ghd7* and *ARE1* alleles by the intro-

Ghd7 enhances rice nitrogen utilization and yield

gression of the *are1-1* allele (in the Nipponbare or NPB background) into various varieties (Supplemental Tables 1 and 2). In these NILs, whereas the *Ghd7* expression was variable, dependent on the specific alleles (Supplemental Figure 1A), the expression of *ARE1* was negatively correlated to that of *Ghd7* (Figure 1A; Supplemental Figure 1A and 1B), suggesting that *Ghd7* negatively regulates *ARE1*. When grown in paddy fields supplied with 300 kg/ha (high nitrogen, HN) or 180 kg/ha (low nitrogen, LN) urea, varieties carrying a null or weak-functional allele of *Ghd7* (*Ghd7-0a* or *Ghd7-2*) had a greater decrease in plant height and grain number than those carrying a strong-functional allele of *Ghd7* (*Ghd7-1* or *Ghd7-3*) under LN growth conditions (Figure 1B and 1C; Supplemental Figure 1C and 1D), suggesting that *Ghd7* confers tolerance to low nitrogen. When a null *are1-1* allele was introduced into these NIL plants, the HN/LN ratio of the plant height and grain number was substantially reduced compared with those carrying a functional *ARE1* allele (*ARE1^{NPB}* or *ARE1^{9311/MH63}*). Moreover, the variations in the HN/LN ratios among the three groups of *Ghd7* alleles were reduced in the *are1-1* background (Figure 1B and 1C; Supplemental Figure 1C and 1D), suggesting that the *Ghd7*-boosted effects were partly dependent on *ARE1*.

It has been shown that the effects of *Ghd7* vary with the genetic background (Xue et al., 2008). Because the above results were obtained in NILs derived from various varieties, we further examined the *Ghd7-ARE1* interaction in a same genetic background with a double-mutant analysis. Three sets of NIL plants were generated in the background of the *japonica* variety Kongyu131 (KY131; genotype *Ghd7-0a ARE1^{NPB}*) by the introgression of a *Ghd7-2* allele and/or an *are1-1* allele derived from the NPB background. For clarity, NIL-*Ghd7-2* (genotype *Ghd7-2 ARE1^{NPB}*), NIL-*Ghd7-2 are1-1* (genotype *Ghd7-2 are1-1*), KY131, and NIL-*are1-1* (genotype *Ghd7-0a are1-1*) were designated as “wild type,” *are1*, *ghd7*, and *ghd7 are1* double mutants, respectively (Figure 1D). Compared with wild type, *ghd7* showed a reduction, whereas *are1* showed an increase, in plant height and grain number under various nitrogen conditions (Figure 1E and 1F; Supplemental Figure 1E). Compared with *Ghd7*, *are1* showed a relatively weak effect on the heading date (Supplemental Figure 1F), implying that *Ghd7* may regulate a broader range of physiological processes than *ARE1*. In response to nitrogen depletion, *Ghd7* expression was induced in a manner opposite that of *ARE1* (Figure 1G). Nitrogen depletion rapidly induced the expression of nitrogen uptake and assimilation genes in the wild-type rice seedlings. However, this induction was reduced in the *Ghd7*-overexpressing plants (*Ghd7-OX*), but was enhanced in the *ghd7* mutant (Figure 1H and 1I; Supplemental Figure 2A–2M). While no significant difference in the Fd-GOGAT activity was observed in the *Ghd7-OX* and *ghd7* plants compared with wild type (Supplemental Figure 3A), the nitrogen uptake rate and NUE were increased in the *Ghd7-OX* plants (Figure 1J and 1K). Compared with wild type, *Ghd7-OX* plants were more tolerant to low nitrogen, associated with the increased expression levels of nitrogen uptake and assimilation genes (Supplemental Figure 3B–3H). A previous study showed that *Ghd7-OX* plants had a decreased chlorophyll level in flag leaves at the heading stage (Wang et al., 2015), which is different from that observed at the late grain-filling stage in this study. Nevertheless, overexpression of *Ghd7* substantially increased grain yield under both HN and LN

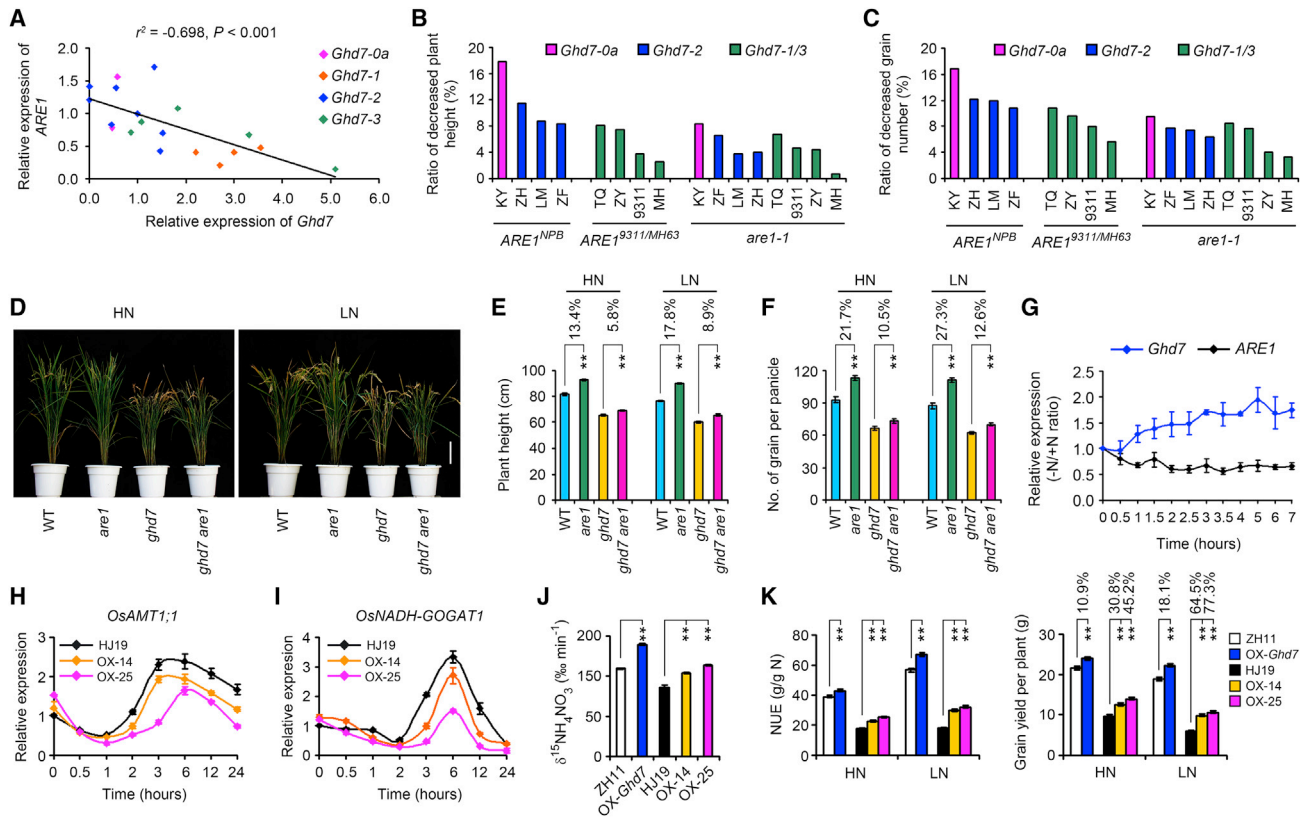


Figure 1. *Ghd7* acts genetically upstream of *ARE1* to modulate nitrogen utilization.

(A) Analysis of the correlation of *ARE1* and *Ghd7* expression in NIL-*are1-1* plants and their recurrent parents carrying various *Ghd7* alleles as specified (see Supplemental Figure 1A and 1B for details). r^2 and P values are determined by the two-way Pearson correlation analysis.

(B and C) Ratios of the decrease in the plant height **(B)** and grain number **(C)** of the indicated plants grown under high (HN; 300 kg/ha urea) or low (LN; 180 kg/ha urea) nitrogen conditions. The ratio was calculated as (HN – LN)/HN (see Supplemental Figure 1C and 1D for details).

(D) Fourteen-week-old plants with the indicated genotypes grown under HN or LN conditions. All plants are in the KY131 genetic background. Scale bar, 15 cm.

(E and F) Quantification of the plant height **(E)** and grain number per main panicle **(F)** of plants shown in **(D)**. Ratios of the increase in plant height and grain number under HN or LN growth conditions are given above the graph. Data presented are mean \pm SEM ($n \geq 20$ plants). ** $P < 0.01$ (Student's t -test).

(G) Analysis of the *Ghd7* and *ARE1* expression mediated by nitrogen. Two-week-old seedlings grown in a nitrogen-containing solution (+N; 1.46 mM NH_4NO_3) were transferred to a nitrogen-free (–N; 0 mM NH_4NO_3) or a nitrogen-containing solution (control; eliminating the effect of circadian rhythm) 2 h after entering the daytime (time 0 h) and culturing was continued for the indicated time. Total RNA prepared from leaves was used for qRT-PCR analysis. Data presented are ratios of the relative expression levels under –N/+N conditions with SEM (three biological repeats; $n \geq 6$ seedlings).

(H and I) Expression of *OsAMT1;1* **(H)** and *OsNADH-GOGAT1* **(I)** in response to nitrogen depletion in wild-type HJ19 and the *Ghd7*-overexpressing seedlings (OX-14 and OX-25) as indicated. The assay was performed as described for **(G)**.

(J) Analysis of nitrogen uptake rate of 2-week-old wild type and the *Ghd7*-overexpressing seedlings grown in the presence of 1.46 mM NH_4NO_3 . Data are mean values of three biological replicates with SEM ($n = 6$ seedlings). ** $P < 0.01$ (ANOVA with Dunnett's test).

(K) Analysis of nitrogen use efficiency (NUE) and grain yield per plant of wild type and the *Ghd7*-overexpressing plants grown under HN (300 kg/ha urea) or LN (180 kg/ha urea) conditions. Ratios of the increase in the grain yield are given above each graph. Data are the mean \pm SEM ($n \geq 40$ plants). ** $P < 0.01$ (ANOVA with Dunnett's test).

conditions (Figure 1K). Collectively, these results suggest that *Ghd7* acts genetically upstream of *ARE1* to regulate nitrogen utilization.

Ghd7 binds the Evening Element-like motifs in *ARE1* to repress its expression

Because *ARE1* expression was increased in *Ghd7-0a*, we reasoned that *Ghd7* may directly or indirectly repress *ARE1* transcription. To test this hypothesis, we examined the putative binding ability of *Ghd7* to the *ARE1* promoter by a yeast one-hybrid assay. Unless specified otherwise, *ARE1* promoter refers to the

sequences of the *ARE1*^{NPB} allele hereafter. The putative promoter, exon 1, and intron 1 of *ARE1* were fused in-frame to an Aureobasidin A resistance gene (*AUR1-C*) to generate a reporter construct (Figure 2A and 2B). Co-transformation of p*ARE1-AUR1-C* with GAD-*Ghd7*, but not with GAD, conferred resistance to Aureobasidin A (Figure 2B), suggesting that *Ghd7* directly binds to *ARE1*. Surprisingly, the deletion of the entire putative *ARE1* promoter up to intron 1 (D1 through D9) did not significantly reduce the resistance of yeast cells to Aureobasidin A (Figure 2B). Further deletion to the 5'-proximal end of intron 1 (D10) dramatically reduced the resistance to Aureobasidin A (Figure 2B), suggesting that *Ghd7* binds to a *cis*

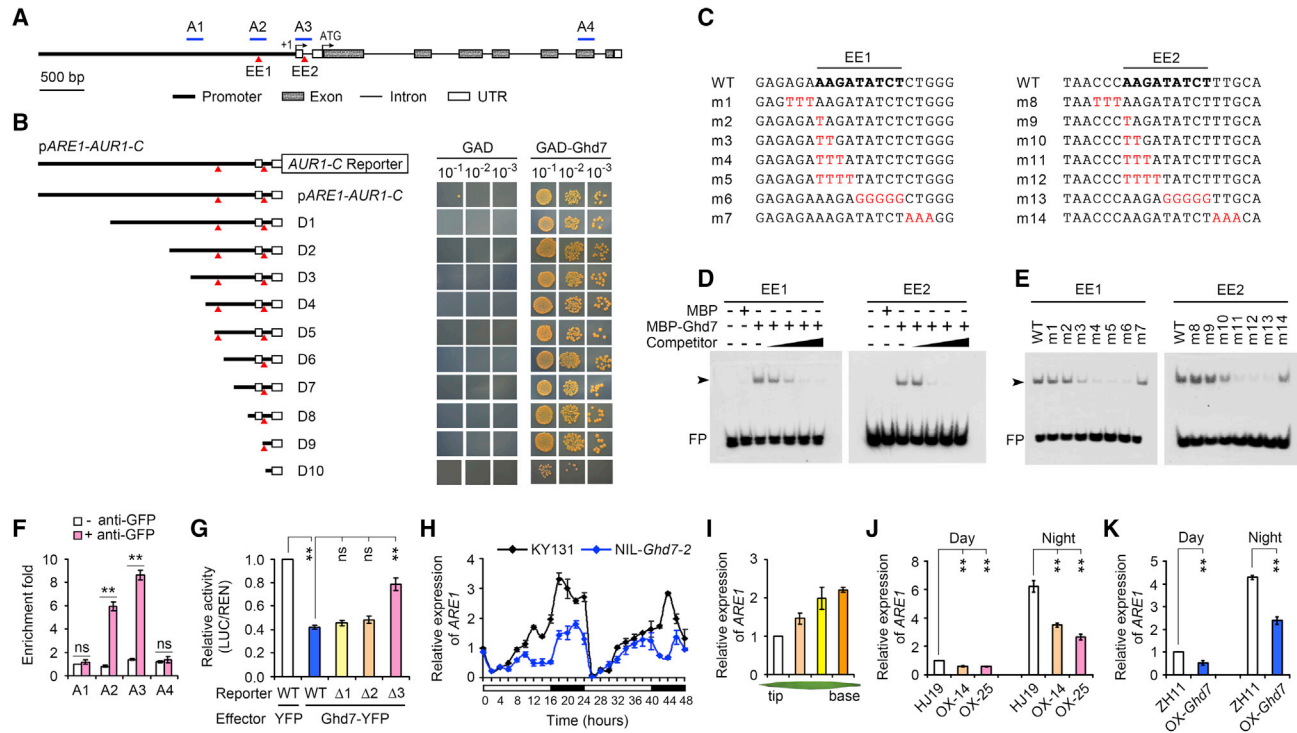


Figure 2. Ghd7 binds two Evening Element-like motifs in *ARE1* and represses its expression.

(A) A schematic map of the *ARE1* gene. Two Evening Element-like motifs (EE1 and EE2) are marked by red triangles and four amplicons (A1–A4) analyzed by chromatin immunoprecipitation (ChIP) are indicated by blue lines. The putative transcription start is referred to as +1.

(B) Left, a schematic map of the *pARE1-AUR1-C* reporter gene is shown on the top; wild-type and mutant (D1–D10) *ARE1* promoters, fused to the *AUR1-C* reporter gene, are shown below. Right, growth of yeast cells co-transformed with the indicated reporter constructs and a pGAD or a pGAD-Ghd7 plasmid as indicated.

(C) Sequences of EE1 and EE2 elements and flanking regions of wild-type (WT) and mutant (m1–m14) probes used in the electrophoretic mobility-shift assay (EMSA). Core sequences of the EEL motifs are shown in bold and the substituted nucleotides are shown in red.

(D and E) EMSA of the purified MBP-Ghd7 recombinant protein (D) and biotin-labeled probes (E) shown in (C). The DNA–protein complex is indicated by arrowheads and free probes are indicated as FP. Un-labeled competitor DNA in (D) is 1-, 20-, 200-, and 500-fold over the labeled probes, respectively.

(F) Analysis of the DNA-binding capability of Ghd7-GFP protein by ChIP. Chromatin sample prepared from *35S::Ghd7-GFP* transgenic plants was immunoprecipitated with or without an anti-GFP antibody and then subjected to qPCR analysis using primer pairs specific to amplicons A1–A4 shown in (A). The relative level in A1 without an anti-GFP antibody is set as 1.0. Data presented are the mean values of four technical replicates with SEM. ***P* < 0.01; ns, not significant (Student's *t*-test).

(G) Analysis of the transcriptional repression activity of Ghd7. A luciferase (LUC) reporter gene driven by wild-type (WT) or mutant ($\Delta 1$ – $\Delta 3$; deletion of EE1, EE2, and both EE1/EE2, respectively) *ARE1* promoters was co-transformed with an effector vector (*35S::YFP* or *35S::Ghd7-YFP*) into rice protoplasts. The LUC activity was measured and normalized to that of the reference reporter REN. The relative LUC activity of the wild-type promoter co-transformed with *35S::YFP* is set as 1.0. Data presented are the mean values of 10 technical replicates with SEM. ***P* < 0.01; ns, not significant (ANOVA with Dunnett's test).

(H) Analysis of diurnal expression profiles of *ARE1* in KY131 (carrying a *Ghd7-0a* allele) and NIL-*Ghd7-2*. Two-week-old seedlings were grown in a nitrogen solution (1.46 mM NH_4NO_3) under long-day conditions (16 h/8 h day/night cycle). Total RNA was prepared from fully expanded leaves in 2 h intervals and used for qRT-PCR analysis. The open and filled boxes under the graph indicate the light and the dark period, respectively.

(I) Analysis of *ARE1* expression levels by qRT-PCR in different segments as indicated of flag leaf blades derived from heading-stage wild-type ZH11 plants at midday. Data are the mean values of three biological replicates with SEM, and each replicate consisted of three plants.

(J and K) Analysis of *ARE1* expression levels in fully expanded leaves of 10-day-old wild-type and *Ghd7*-overexpressing seedlings by qRT-PCR; leaves were collected 4 h after entering daytime or nighttime. Data presented in (H), (J), and (K) are the mean values of three technical replicates with SEM (*n* ≥ 6 plants). ***P* < 0.01 (Student's *t*-test).

element in this region. Inspection of this region using the PLACE database (Higo et al., 1999) revealed the presence of two perfect palindromic EEL motifs (5'-AAGATATCT-3') (Harmer et al., 2000) in the promoter and intron 1 (Figure 2A and 2C), which were designated as EE1 and EE2, respectively.

In an electrophoretic mobility-shift assay (EMSA), MBP-Ghd7 recombinant protein was capable of efficiently binding to two biotin-labeled DNA fragments containing EE1 or EE2, and the

binding activity was inhibited by the biotin-free DNA fragments in a dose-dependent manner (Figure 2C and 2D). Moreover, the disruption of the core EEL sequences abolished their binding by MBP-Ghd7 recombinant protein (Figure 2C and 2E). Taken together, these results suggest that Ghd7 binds to two EEL motifs in the promoter and intron 1 of the *ARE1* gene.

We next performed a chromatin immunoprecipitation (ChIP) coupled with quantitative PCR (qPCR) analysis in transgenic

Ghd7 enhances rice nitrogen utilization and yield

Molecular Plant

KY131 plants overexpressing a *Ghd7-GFP* transgene (Supplemental Figure 4A and 4B). Among four analyzed amplicons in *ARE1* (A1–A4; see Figure 2A), the signals specific to the anti-GFP antibody were highly enriched in amplicons A2 and A3, which cover EE1 and EE2, respectively (Figure 2F), suggesting that Ghd7-GFP binds to these two motifs *in planta*. In a transient expression assay in mesophyll protoplasts, the luciferase activity of an *ARE1::Luc* reporter gene was reduced to ~40% when co-transformed with a 35S::*Ghd7-YFP* effector vector compared with that of a 35S::*YFP* vector (Figure 2G and Supplemental Figure 4C), suggesting that Ghd7-YFP represses the expression of *ARE1::Luc*. The deletion of either EE1 or EE2 ($\Delta 1$ or $\Delta 2$) did not have an apparent effect on the Ghd7-YFP-repressed expression of *ARE1::Luc*. However, the deletion of or substitution in both EE1 and EE2 significantly relieved the expression of *ARE1::Luc* from the Ghd7-YFP-mediated repression (Figure 2G; Supplemental Figure 4C–4E), suggesting that either element is sufficient for the Ghd7-mediated transcriptional repression. We noticed that the reduced *ARE1* expression in *ARE1*⁹³¹¹ and *ARE1*^{MH63} alleles may not be directly related to Ghd7 (Supplemental Figure 4F). These results suggest that Ghd7 directly binds to two EEL motifs in the *ARE1* promoter and intron 1 to repress the transcription of *ARE1*.

While the EE motif has been shown to function as a *cis* element regulating circadian oscillation expression of genes (Harmer et al., 2000), the expression of *Ghd7* shows a diurnal oscillation pattern (Xue et al., 2008). As a downstream component of *Ghd7*, *ARE1* also displayed a diurnal oscillation pattern opposite that of *Ghd7* (Figure 2H). Compared with KY131 (containing a *Ghd7-0a* null allele), NIL-*Ghd7-2* (containing a weakly functional allele) plants exhibited a reduced amplitude of *ARE1* diurnal oscillation (Figure 2H). Consistent with the above results, *ARE1* showed a gradient expression pattern from the base (high) to the tip of a leaf (Figure 2I and Supplemental Figure 4G), opposite that of *Ghd7* (Weng et al., 2014). Moreover, overexpression of *Ghd7* substantially repressed the *ARE1* expression compared with wild-type plants during both daytime and nighttime (Figure 2J and 2K; Supplemental Figure 4H–4J). We noticed that the expression of the *Ghd7* transgene, driven by a constitutive maize ubiquitin promoter and the *Ghd7* native promoter in HJ19 and ZH11, respectively (Weng et al., 2014), showed a differential expression pattern during daytime and night (Supplemental Figure 4H–4J). Nevertheless, while the regulatory mechanism of this differential expression pattern remains elusive, the expression of *ARE1* showed a pattern opposite that of *Ghd7* during both daytime and nighttime (Figure 2J and 2K). We also noticed that the *ARE1* expression was not completely repressed in the *Ghd7*-overexpressing plants (Figure 2J and 2K), similar to what was observed in the protoplast transient expression assay (Figure 2G), suggesting that *ARE1* may also be regulated by other transcriptional regulators. Taken together, these results suggest that *Ghd7* negatively regulates the *ARE1* expression in a diurnal oscillated manner.

Ghd7 and ARE1 might be subjected to diversifying selection during breeding

To examine if *Ghd7* and *ARE1* are artificially selected during breeding, we performed a geographical distribution analysis of the allelic variants of these two genes, using a panel of 233 vari-

eties cultivated in a wide geographical range in East and South Asia. For conciseness, the strong-functional *Ghd7-1* and *Ghd7-3* alleles (*Ghd7-1/3*) and the weak-functional *Ghd7-2* and non-functional *Ghd7-0/0a* alleles (*Ghd7-0/2*) were grouped into two classes in the following analyses. We found that the geographical distribution of these varieties showed a distinctive pattern roughly divided by 30° north. Along this line, varieties carrying the *Ghd7-1/3* group (80.3%) and the *Ghd7-0/2* group (46.0%) were mainly cultivated in the south and north of 30° north, respectively (Figure 3A and Supplemental Table 3). Remarkably, the distribution of the strong-functional *ARE1*^{NPB} allele (84.0%) and the weak-functional *ARE1*^{9311/MH63} alleles (60.1%) displayed a reversed pattern, also along 30° north, respectively (Figure 3B and Supplemental Table 3). These observations suggest that both *Ghd7* and *ARE1* have likely been subjected to artificial selection during breeding.

What are the possible driving forces for the observed geographical distribution patterns of the *Ghd7* and *ARE1* alleles? While the geographical distribution of the *Ghd7* alleles is likely related to the heading date for the environmental adaptability (Xue et al., 2008), we asked if nitrogen is a driving force for the selection of *Ghd7* and *ARE1* alleles. Previous studies showed that the NDR in soil varied significantly in East and South Asia (Galloway et al., 2004, 2008; Dentener et al., 2006). Based on these results, we roughly divided these areas into three categories, NDR <10, 10–30, and >30 kg/ha per year (Supplemental Figure 5A). Strikingly, varieties carrying the *Ghd7-1/3* (over 90%) or *ARE1*^{9311/MH63} (over 98%) alleles were grown in areas with NDR lower than 30, of which more than 46% and 64% of these two types of alleles were in areas with NDR lower than 10 (Figure 3A–3C; Supplemental Figure 5A and Supplemental Table 3), suggesting that *Ghd7-1/3* and *ARE1*^{9311/MH63} represent elite alleles conferring tolerance to low-nitrogen conditions. By contrast, varieties carrying the *Ghd7-0/2* (25%) or *ARE1*^{NPB} (27%) alleles were grown in areas with NDR higher than 30 (Figure 3C and Supplemental Figure 5A). These results suggest that the elite alleles of both *Ghd7* and *ARE1* had likely undergone strong selection during breeding at the lower latitude areas, associated with the nitrogen deposition levels in soil.

Given that *Ghd7* and *ARE1* were likely selected during breeding, we then asked if they had been subjected to co-selection. To this end, we analyzed the allelic distribution of *Ghd7* and *ARE1* in a panel of 2656 varieties reported in the 3K Rice Genomes Project (Zheng et al., 2015; Wang et al., 2018b, 2020). Among the analyzed varieties, whereas a small fraction was *Ghd7-0* (47 hits; 1.8%) and *Ghd7-0a* (4 hits; 0.2%), the majority were identified as the weak allele *Ghd7-2* (969 hits; 36.5%) and the strong-functional alleles *Ghd7-1* (1486 hits; 55.9%) and *Ghd7-3* (150 hits; 5.6%) (Supplemental Figure 5B). Similar to what was observed previously (Xue et al., 2008), most of the *Ghd7-1* and *Ghd7-3* alleles were found in *indica* varieties, whereas the weak allele *Ghd7-2* was mainly found in *japonica* varieties (Supplemental Figure 5B). For *ARE1*, three major alleles have been identified, which are classified into *ARE1*^{NPB} (81.4%) and *ARE1*^{9311/MH63} (18.6%) groups (Figure 3D).

We then analyzed the distribution of the allelic variants of *Ghd7* and *ARE1* with four different combinations (Figure 3D). Groups I, II, and IV, harboring one or both of the elite alleles of *Ghd7-1/3*

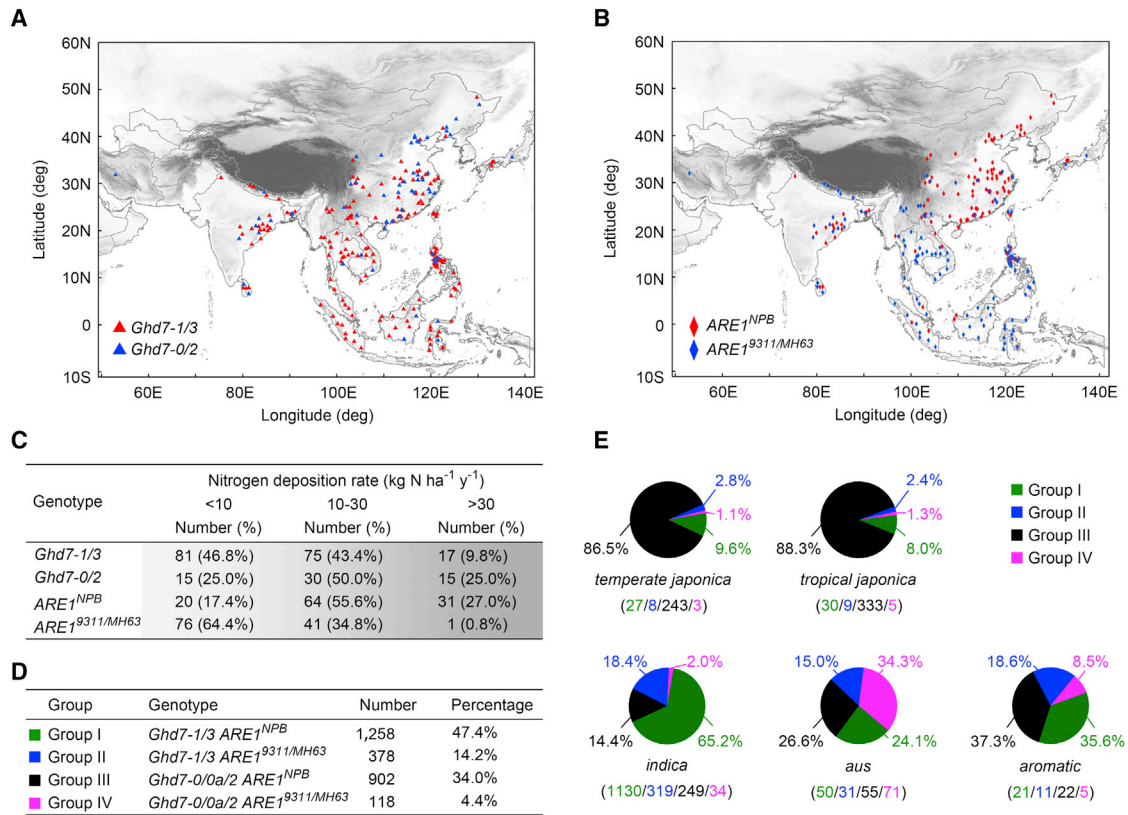


Figure 3. Ghd7 and ARE1 might undergo diversifying selection during breeding.

(A and B) Geographic distribution of major natural alleles of *Ghd7* (A) and *ARE1* (B). A core collection of 233 rice varieties carrying various *Ghd7* and *ARE1* alleles representing a broad range of rice germplasm was used to mark geographic distribution in the main rice cultivation regions in East and South Asia. For conciseness, the strong *Ghd7-1/Ghd7-3* alleles, the null and weak *Ghd7-0/Ghd7-2* alleles, and the weak *ARE1⁹³¹¹/ARE1^{MH63}* alleles are grouped together.

(C) Distribution of *Ghd7* and *ARE1* haplotypes in different regions with various soil nitrogen deposition rates (NDRs). The increased intensity of the background indicates the increased nitrogen concentrations in soil. See also Supplemental Figure 5A for geographical distribution of NDR.

(D) Classification and haplotype abundance of various combinations of *Ghd7* and *ARE1* alleles in a panel of 2656 rice varieties.

(E) Distribution of Groups I–IV specified in (D) in different rice subpopulations. Number and percentage of each group in a given subpopulation are shown.

and/or *ARE1^{9311/MH63}*, were mainly present in the *indica* (85.6%) varieties, but dramatically reduced to 11.7%–13.5% in the *japonica* varieties (Figure 3D and 3E), which generally showed less efficient nitrogen utilization than other varieties (Ta and Ohira, 1981; Hu et al., 2015; Wang et al., 2018a; Gao et al., 2019). Conversely, Group III, carrying both *Ghd7-0/0a/2* and *ARE1^{NPB}* alleles, was found to be dominant in *japonica* varieties (over 86%) but with relatively lower frequency in *aus* (26.6%), *aromatic* (37.3%), and *indica* (14.4%) varieties (Figure 3D and 3E), suggesting that *Ghd7* and *ARE1* constitute important contributors of NUE. In a linkage disequilibrium analysis, we found that *Ghd7-1/3* and *ARE1^{9311/MH63}* alleles, and *Ghd7-0/0a/2* and *ARE1^{NPB}* alleles, tended to be associated with each other ($D' = 0.38$, $P = 3.5 \times 10^{-14}$, Fisher's exact test), respectively. Since these two genes are located on different chromosomes, this result suggests that *Ghd7* and *ARE1* had co-evolved, likely driven by diversifying selection during breeding.

Improvement of NUE by selective combination of elite alleles of *Ghd7* and *ARE1*

Data presented above suggest that the *Ghd7* and *ARE1* alleles have undergone diversifying selection during breeding, while the

occurrence of both elite alleles of *Ghd7-1/3* and *ARE1^{9311/MH63}* is at low frequency. We thus reasoned that the combination of elite alleles of *Ghd7* and *ARE1* may provide a useful approach for the improvement of rice. To explore this possibility, we introduced the *ARE1⁹³¹¹* or *ARE1^{MH63}* weak allele into NPB plants that carry a strong *ARE1^{NPB}* allele and a weak *Ghd7-2* allele (Figure 4A and Supplemental Figure 6A). Compared with NPB, the NIL-*ARE1⁹³¹¹* and NIL-*ARE1^{MH63}* plants were more tolerant to LN conditions than NPB and produced more grains (Figure 4B and 4C; Supplemental Figure 6B–6F). Consequently, the grain yield of NIL-*ARE1⁹³¹¹* and NIL-*ARE1^{MH63}* plants was increased by 10.2%–28.4% and 10.4%–26.2%, respectively, compared with NPB plants under LN conditions (Figure 4D). We noticed that NIL-*ARE1⁹³¹¹* and NIL-*ARE1^{MH63}* plants delayed the heading date for ~2 days without apparent effects on the mature time and grain weight, while the *are1-1* plants usually delayed the heading date by ~4 days and mature time by 7–10 days (Supplemental Figure 6A, 6G, and 6H).

For the low-latitude cultivation regions with longer growing season and lower soil nitrogen concentration, the main cultivars are *indica*, generally carrying strong-functional alleles

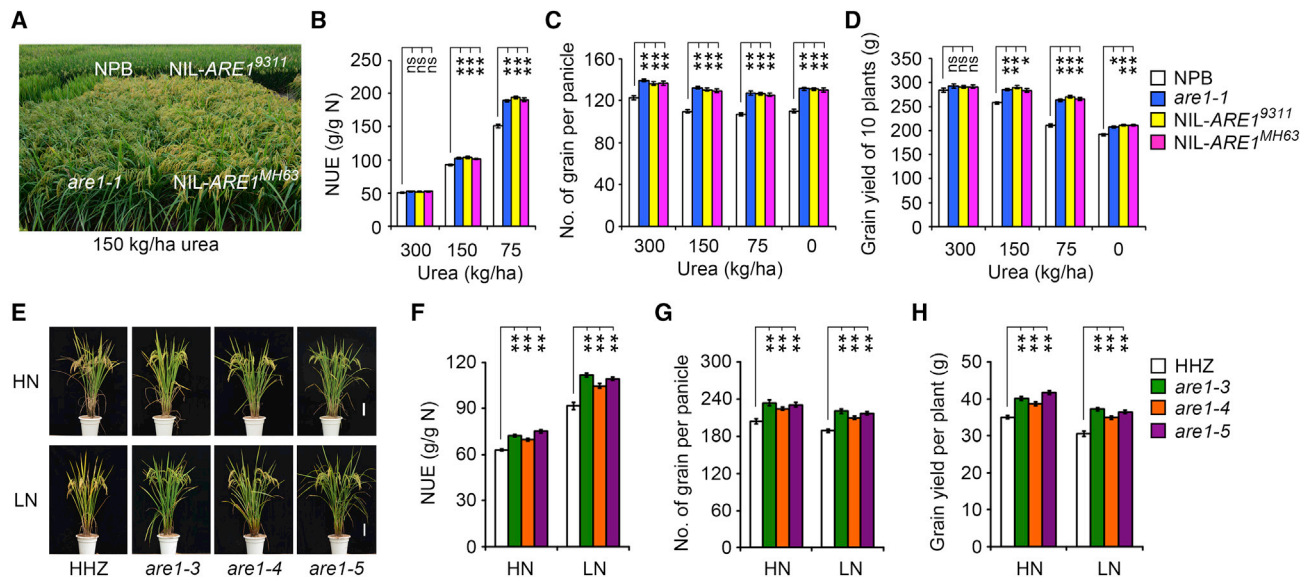


Figure 4. Improvement of NUE by combination of elite *ARE1* and *Ghd7* alleles.

(A) Field-grown rice plants with the indicated genotypes at the mature stage. See Supplemental Figure 6A for plants grown under other nitrogen conditions.

(B–D) Analysis of nitrogen use efficiency (NUE) (B), grain number per main panicle (C), and grain yield (D) of indicated plants grown under various urea concentrations.

(E) Rice plants with the indicated genotypes grown under high (HN; 300 kg/ha urea) or low (LN; 180 kg/ha urea) nitrogen conditions. The *are1-3* through *are1-5* mutants were generated by CRISPR-Cas9-based genome editing in the HHZ background. Scale bars, 15 cm.

(F–H) Analysis of NUE (F), grain number per main panicle (G), and grain yield (H) of plants shown in (E).

Data in (B) and (D) are mean values of eight replicates with SEM. Data in (C) and (F–H) are mean ± SEM ($n \geq 40$ plants). * $P < 0.05$; ** $P < 0.01$; ns, not significant (ANOVA with Dunnett’s test).

of *Ghd7-1/3* and/or weak alleles of *ARE1*^{9311/MH63}. We asked if the introduction of an *are1* null allele into the *Ghd7* strong-functional allele background could further improve NUE and increase grain yield. We tested this idea in Huanghuazhan (HHZ; carrying *Ghd7-3* and *ARE1*⁹³¹¹ alleles), one of the widely cultivated high-yield *indica* varieties in the South China areas, where NDR in soil is relatively low. We generated and characterized three null-mutant *are1* alleles (*are1-3* through *are1-5*) using CRISPR-Cas9-based genome editing in the HHZ background (Supplemental Figure 7A and 7B). Compared with wild-type HHZ plants, *are1-3* through *are1-5* plants showed improved NUE and nitrogen-regulated traits under LN conditions (Figure 4E–4G and Supplemental Figure 7C–7G). Similar to *are1-1*, the heading date of *are1-3* through *are1-5* was delayed by 2–3 days and the grain weight was slightly decreased (Supplemental Figure 7H and 7I). Nevertheless, the grain yield of *are1-3* through *are1-5* plants was increased by 10.4%–21.8% compared with HHZ under both HN and LN conditions (Figure 4H). Taken together, the above results demonstrate that the combination of elite alleles of *ARE1* and *Ghd7* is an effective approach for the improvement of NUE and to boost grain yield in breeding.

The rice *Ghd7* gene is a master regulator of various important agronomic traits, including plant height, heading date, grain number, and stress responses. In this study, we find that *Ghd7* positively regulates NUE. The transcriptional repressor *Ghd7* directly binds to two EEL motifs in *ARE1*, a negative regulator of NUE, to repress its expression. As two components in a linear genetic pathway, *Ghd7* and *ARE1* might have co-evolved, driven by

diversifying selection during breeding, which is closely associated with the NDR in soil. Moreover, we also show that the combination of elite alleles of *ARE1* and *Ghd7* substantially improves NUE and grain yield. These discoveries define an unrecognized mechanism regulating nitrogen utilization and its associated agronomic traits, thus providing a useful approach for the improvement of grain productivity in rice.

The *Ghd7*-regulated traits are largely associated with those modulated by nitrogen. *Ghd7* is characterized as an important regulator of NUE in this study, consistent with the notion that *Ghd7* is identified as a causal locus for nitrogen in a genome-wide association study (Yang et al., 2018). What are the targets of *Ghd7* in regulating NUE? We show that *Ghd7* acts genetically upstream of *ARE1* to repress its expression. Because mutations in both EE1 and EE2 are necessary to relieve the suppression on *ARE1*, *Ghd7* may bind to these two elements in a cooperative fashion. Moreover, because EE1 and EE2 are separated by a distance of 366 bp, it is likely that the *Ghd7*-bound EE1 and EE2 are tethered together to form a stable complex, which may stall the assembly of the pre-initiation complex or impede the load of the pre-initiation complex onto the promoter (Supplemental Figure 8). The presumably cooperative mechanism of EE1 and EE2 requires a relatively high concentration of *Ghd7* protein to ensure the effective occupancy of both elements, which may fit the diurnal regulation of *Ghd7* on *ARE1* in a more efficient manner. This reciprocal-regulated diurnal oscillation of the *Ghd7-ARE1* module may play an important role in regulating the utilization and metabolism of nitrogen and perhaps carbon in response to

Molecular Plant

alternating day and night. We notice that multiple putative *cis* regulatory elements are found in the *ARE1* promoter, including two CCA1-binding sites and two SORLIP1 motifs that are involved in the regulation of circadian- and light-regulated genes (Wang et al., 1997; Hudson and Quail, 2003; Jiao et al., 2005), respectively, suggesting that the transcription of *ARE1* is regulated by multi-layered mechanisms. In a more extended view, *VRN2*, the wheat ortholog of *Ghd7*, is directly repressed by the *VRN1* transcription repressor in regulating flowering (Chen and Dubcovsky, 2012; Deng et al., 2015), implying that the regulatory scheme of the *Ghd7-ARE1* pathway is more complicated than that discovered in this study.

As two important regulators of the NUE-associated traits, *Ghd7* and *ARE1* have been subjected to diversifying selection during breeding, and the selection shows a strong correlation with the soil-deposited nitrogen level, consistent with the observation that the geographical distribution of *TCP19*, a key regulator for NUE, is also closely correlated to NDR in soil (Liu et al., 2021). However, the co-selection of elite alleles of these two loci is at a relatively low frequency. This is likely because these two loci function in a linear pathway to regulate similar agronomic traits, rendering it suitable for the selection of either locus during breeding. Moreover, the physiological processes regulated by these two genes are also significantly divergent (Xue et al., 2008; Weng et al., 2014; Wang et al., 2018a; Yang et al., 2018). The combined elite alleles of *Ghd7* and *ARE1* substantially increased NUE and grain productivity under low-nitrogen growth conditions in both high- and low-latitude varieties, indicating that this is a useful approach in breeding. Finally, because both *Ghd7* and *ARE1* are highly conserved in flowering plants (Ream et al., 2012; Yang et al., 2012; Woods et al., 2016; Wang et al., 2018a), the combination of elite alleles of these two genes may also offer a practical approach for the genetic improvement of NUE and productivity in other crops.

METHODS

Plant materials and growth conditions

Rice varieties used in this study and their genotypes related to *Ghd7* and *ARE1* loci are listed in Supplemental Tables 1 and 2. All NIL^{*are1-1*} plants were constructed by backcrossing of the *are1-1* mutant (in the NPB background) with its recurrent parents six to nine times, and the resulting BC₅₋₈F₄ plants were used in this study. The NIL-*Ghd7-2 are1-1* plant was constructed by crossing NIL-*are1-1* and NIL-*Ghd7-2* and the resulting F₃ plants were used. The *are1-3* through *are1-5* null alleles in the HHZ background were obtained by CRISPR-Cas9-based genome editing (see also below for plasmid construction). The primary transformants were backcrossed to wild-type HHZ three times and *are1/are1 Cas9*-free BC₂F₃ plants were selected for the analysis. The *Ghd7*-overexpressing transgenic plants (Weng et al., 2014) were kindly provided by Drs. Qifa Zhang and Yongzhong Xing.

Genetic transformation of rice plants was performed using *Agrobacterium*-mediated methods as described previously (Wang et al., 2018a).

Hydroponic cultivation was performed in a greenhouse as described previously (Wang et al., 2018a). For the analysis of diurnal gene expression patterns, seedlings were grown in a growth chamber with 70% relative humidity under 16 h/8 h light/dark and 25°C–30°C/25°C day/night conditions. Field-cultivated plants were grown during the routine rice growing season at the Experimental Station of the Institute of Genetics and Developmental Biology located in Beijing (40°13'N, 116°37'E); Ling-

Ghd7 enhances rice nitrogen utilization and yield

shui, Hainan province (18°31'N, 110°01'E); and the Experimental Station of the Shandong Rice Research Institute located in Jinan, Shandong province (37°03'N, 117°14'E).

Field trial

A randomized block design approach was adopted to arrange replicates/plots/plants for the field trial in Jinan. All plants were equally cultivated with a distance of 15 × 25 cm in a 4.0 × 4.0 m plot, and each line consisted of at least 100 plants. Urea was used as the only nitrogen source, applied at the seedling, the tillering, and the booting stages, with 30%, 40%, and 30% of the total applied urea at each stage, respectively. Potassium sulfate (120 kg/ha) and calcium phosphate (260 kg/ha) were used as potassium and phosphorus fertilizers, respectively, and supplied during rice transplanting. Statistical analysis of the plant height, tiller number, 1000-grain weight, grain number, and grain weight was conducted when all lines in the same genetic background reached the mature stage. The soil-plant analysis development (SPAD) value was measured using a handheld digital meter (SPAD-502, Minolta Camera Co., Osaka, Japan), and data were collected by measuring the middle area of a flag leaf in one genetic background. All field trials were repeated for at least three seasons and similar results were obtained.

Plasmid construction

Plasmids were constructed following standard molecular cloning methods (Green and Sambrook, 2012). The *Ghd7-1* coding sequence was PCR amplified using MH63 cDNA as a template and primer pairs were embedded with *Bam*HI/*Eco*RI sites and cloned into the *Eco*RV site of a pBluescript-SK vector (Stratagene) to yield pSK-Ghd7be. To construct pMBP-Ghd7, the *Ghd7-1* cDNA fragment released by *Bam*HI/*Eco*RI digestion was inserted into the same sites of pMAL-c2X (New England Biolabs).

To construct the prey vector used in the yeast one-hybrid assay, the *Ghd7-1* cDNA fragment in pSK-Ghd7be, constructed similar to pSK-Ghd7be, was released by *Eco*RI/*Bam*HI digestion and then inserted into the same sites of a pGADT7 vector (Clontech) to generate pGAD-Ghd7. To construct the *ARE1* promoter-based reporter vector, a 2000 bp DNA fragment spanning nucleotides –1584 to +416 (the putative transcription start is referred to as +1) of the *ARE1* gene was PCR amplified using the Nipponbare genomic DNA as a template and primer pairs embedded with *Sac*I/*Kpn*I restriction sites. The PCR fragment was cloned into the *Eco*RV site of a pBluescript-SK vector to yield pSK-ARE1sk. The *ARE1* fragment released by *Sac*I/*Kpn*I digestion was inserted into the same sites of pAbAi (Clontech) to yield the pARE1-AUR1-C reporter construct. A similar approach was applied to construct the D1–D10 mutants (see Figure 2B), which truncate from the 5'-proximal side at –1584 to the following positions: –1084 (D1), –604 (D2), –384 (D3), –284 (D4), –184 (D5), –84 (D6), +17 (D7), +117 (D8), +217 (D9), and +233 (D10).

To construct the pARE1-LUC reporter vector, a similar intermediate construct, pSK-ARE1kn, was made, which was flanked by *Kpn*I and *Nco*I sites. The *ARE1* fragment released by *Kpn*I/*Nco*I digestion was cloned into the same sites of a pGreenII 0800-LUC vector (Hellens et al., 2005) to yield pARE1-LUC (the NPB version), pARE1-LUC93 (the 9311 version), and pARE1-LUCmh (the MH63 version). Deletion and substitution mutations were made using pARE1-LUC (the NPB version) as a backbone and the Fast Mutagenesis System (Transgen; cat. no. FM111-02) following the manufacturer's instructions. A pSK-Ghd7hs intermediate vector was constructed using an approach similar to that of pSK-Ghd7be, which was flanked by *Hind*III and *Sac*I sites. A *Hind*III/*Sac*I fragment released from pSK-Ghd7hs was inserted into the same sites of a pSAT6-EYFP-N1 vector (Tzfira et al., 2005) to produce p35S::Ghd7-YFP.

To construct the p35S::Ghd7-GFP binary vector, an 813 bp fragment was PCR amplified using NPB cDNA as a template and primer pairs embedded

Ghd7 enhances rice nitrogen utilization and yield

with *SpeI/PmlI* restriction sites, and then inserted into a pCAMBIA1305-GFP vector by homologous recombination used for the genetic transformation of rice KY131 plants.

To construct the pCRISPR-Cas9-*ARE1* plasmids, three sgRNA target sites (nucleotides +501 to +523, +1636 to +1658, and +2861 to +2883, located in the first, second, and fifth exon of *ARE1*, respectively; the putative transcription start is referred to as +1) with 5'-G(N)₁₉NTNGG (the putative spacer adjacent motif) features were manually selected. A nucleotide BLAST method against the rice genome sequence was performed to confirm targeting specificity in the rice genome. To construct the sgRNA expression cassette harboring the Target 1 sequence, a pYLsgRNA-U6a vector (Ma et al., 2015) was linearized by *BsaI* and ligated to a double-stranded adaptor of Target 1 (Invitrogen). The ligated product was PCR amplified using primer pair U_F/gRNA_R for 28 cycles and then used as the template for a secondary PCR amplification using the site-specific primer pair U6a_F/U6a_R embedded with *BsaI* restriction sites. Another two sgRNA expression cassettes harboring Target 2 and Target 3 sequences driven by the U6b and U6c promoters, respectively, were constructed using a similar approach. Three sgRNA expression cassettes were simultaneously cloned into the *BsaI* sites of a pYLCRISPR/Cas9-MH vector (Ma et al., 2015).

All constructs were verified by extensive restriction digestion and DNA-sequencing analysis. Sequences of all primers used in the cloning are listed in Supplemental Table 4.

Quantitative RT-PCR

Total RNA was prepared from leaves or roots using an RNAPrep Pure Plant Kit (TIANGEN; cat. no. DP432). RNA samples were treated with DNase I for 10 min at room temperature and then used as templates for cDNA synthesis using a TransScript First-Strand cDNA Synthesis Super-Mix (Transgen; cat. no. AT301) following the manufacturer's instructions. qPCR was performed using an UltraSYBR Mixture (CWBIQ; cat. no. CW2601M) in a CFX96 Real-Time System (BIO-RAD, USA). To examine the diurnal expression of *ARE1*, rice seedlings were subjected to long-day (16 h/8 h day/night cycle) conditions for 2 week training, and then leaf blades were excised at 2 h intervals of two day/night cycles and used for the qPCR analysis. The rice *Ubiquitin 1* (*UBQ*; Os03g0234200) gene was used as an internal control for normalization. Sequences of all the primers used in qPCR are listed in Supplemental Table 4.

Yeast one-hybrid assay

The yeast one-hybrid assay was performed using a Matchmaker Gold Yeast One-Hybrid System (Clontech; cat. no. 630491) following the manufacturer's instructions. The transformed yeast cells with various reporter vectors were plated on SD/-Ura medium for 48 h and the positive clones were identified by colony PCR. The effector vectors were transformed into the reporter strains and plated on SD/-Leu medium for 48–72 h. The positive strains were randomly selected, serially diluted (1/10, 1/100, and 1/1000), and then plated onto SD/-Leu medium with or without 500 ng/ml Aureobasidin A. After culturing for 48–72 h, the plates were observed and photographed.

Electrophoretic Mobility-Shift Assay

A pMBP-Ghd7 expression vector was transformed into the *E. coli* Rosetta (DE3) strain. The expression and purification of MBP-Ghd7 recombinant protein were performed using amylose resin beads (New England Biolabs; cat. no. E8021S) following the manufacturer's instructions.

EMSA was performed using a LightShift Chemiluminescent EMSA Kit (Thermo Scientific; cat. no. 20148) following the manufacturer's instructions. Briefly, the complementary oligonucleotides labeled with biotin at the 5' end were synthesized (Invitrogen) and annealed. Approximately 500 ng of protein and 200 pM biotin-labeled probes were incubated in 20 μ l of reaction mixtures (10 mM Tris-HCl [pH 7.5], 50 mM KCl, 1 mM

Molecular Plant

DTT, 2.5% glycerol, and 5 ng/ μ l poly(dI-dC)) for 20 min at room temperature. The reaction was then separated on a 6% polyacrylamide gel in 0.5 \times TBE buffer (45 mM Tris, 45 mM boric acid, 1 mM EDTA [pH 8.3]). Biotin-free probes with various dilutions were added to the reactions for the competition with biotin-labeled DNA target. The DNA-protein binding was detected by chemiluminescence in a film cassette.

Protoplast transient expression assay

Preparation of protoplasts and poly(ethylene glycol)-mediated transfection were performed as described previously (Wang et al., 2018a). Briefly, the reporter and effector constructs were co-transformed into protoplasts prepared from leaf sheath of KY131 seedlings. The transfected protoplasts were incubated at 24°C for an additional 18–20 h to allow the expression of the introduced genes. Afterward, the bioluminescence was measured using a Dual-Lucy Assay Kit (Vigorous; cat. no. T002) in a GloMax 20/20 luminometer (Promega) following the manufacturer's instructions. A *Renilla* (*REN*) luciferase reporter gene, driven by the CaMV 35S promoter and embedded in the pGreenII 0800-LUC vector (Hellens et al., 2005), was used as a reference for the transfection efficiency. The LUC activity was normalized to the REN activity in all reporter analyses. For all transient expression, at least four independent transformations were performed and the average values with the standard error of the mean (SEM) are presented.

Immunoblotting analysis

Approximately 2 g of fresh plant material was ground into a fine powder in liquid nitrogen and suspended in 1 ml of cold extraction buffer (50 mM Tris-HCl [pH 7.5], 150 mM NaCl, 10 mM MgCl₂, 0.1% NP-40, and 1 mM PMSF). The sample was cleaned twice by centrifugation at 12 000 g at 4°C for 10 min. The supernatant was collected and protein concentration was determined using the Bradford assay. Typically, ~20 μ g of protein sample was mixed with 1/4 volume of 5 \times loading buffer (1 M Tris-HCl [pH 6.8], 50% glycerol, 10% SDS, 5% β -mercaptoethanol, and 5% bromophenol blue), boiled for 5–10 min, and then electrically separated on SDS-PAGE at 120 V for 2–3 h. After electrophoresis, proteins were electrically transferred onto a 0.45 μ m polyvinylidene fluoride membrane. After the transfer, the membrane was incubated with a primary antibody (mouse monoclonal anti-GFP antibody, Abmart; cat. no. M2000L, 1:20 000 dilution; mouse anti-HSP82 antibody, Beijing Protein Innovation; cat. no. AbM51099-31-PU, 1:25 000 dilution) for 1–2 h. After a wash, the membrane was incubated with a horseradish peroxidase-goat anti-mouse IgG antibody (Beijing Dingguo Changsheng Biotech; cat. no. IH-0031, 1:100 000 dilution) for 1–2 h. The signal was detected using a SuperSignal West Femto Maximum Sensitivity Substrate kit (Thermo Scientific; cat. no. 34096) following the manufacturer's instructions.

Chromatin immunoprecipitation assay

ChIP assay was performed as described previously (Saleh et al., 2008) with modifications. Briefly, approximately 5 g of flag leaf blades was cut into small pieces and immediately fixed in 45 ml of cross-linking buffer (400 mM sucrose, 10 mM Tris-HCl [pH 8.0], 1 mM PMSF, 1 mM EDTA, and 1% formaldehyde) under vacuum filtration with pressure of 0.67 kg/cm² for 10 min. After the cross-linking, 3.3 ml of 2 M glycine was added to a final concentration of 125 mM and incubated for an additional 5 min at room temperature. The sample was washed three times with sterile deionized water, the water drained with paper tissues, and the sample ground into a fine powder with liquid nitrogen. The sample was then resuspended in 25 ml of freshly made nuclear isolation buffer (250 mM sucrose, 15 mM PIPES [pH 6.8], 5 mM MgCl₂, 60 mM KCl, 15 mM NaCl, 1 mM CaCl₂, 1% Triton-X 100, 1 mM PMSF, and 1 mg/ml Roche Complete protease inhibitor cocktail), vortexed briefly, and incubated for 30 min at 4°C with gentle rotation or shaking, and then passed through four layers of Miracloth. After the filtration, the nuclear sample was pelleted by centrifugation at 11 000 g for 20 min at 4°C, followed by resuspension in 3 ml of fresh cold lysis buffer (50 mM HEPES [pH 7.5], 150 mM NaCl, 1 mM EDTA, 1% SDS, 0.1% sodium deoxycholate, 2% Triton-X 100, 0.1 mM

Molecular Plant

PMSF, and 1 mg/ml Roche Complete protease inhibitor cocktail). The preparation was divided into four aliquots and then subjected to sonication by sonicating 15 times for 10 s/60 s on/off cycle at power Low 4 using a Diagenode Bioruptor Next Gen system, which results in the generation of 200–1000 bp DNA fragments. After the sonication, the sample was cleared by centrifugation at 13 800 *g* for 10 min at 4°C, and the supernatants were collected and combined, and then approximately five-fold diluted with fresh dilution buffer (50 mM HEPES [pH 7.5], 150 mM NaCl, 1 mM EDTA, 0.1% sodium deoxycholate, 0.1% Triton X-100, 0.1 mM PMSF, and 1 mg/ml Roche Complete protease inhibitor cocktail). To pre-clear the chromatin sample, the supernatant was further centrifuged twice at 16 000 *g* for 10 min at 4°C and then incubated with 4% of volume protein-A agarose beads (25% pre-equilibrated slurry) for 90 min at 4°C on a rotating wheel. The sample was centrifuged at 3800 *g* for 2 min at 4°C and the supernatant was collected.

The sample prepared as described above was divided equally into two parts for subsequent experiments, while approximately 1% of the sample was saved to serve as an input control. The two divided samples were incubated with a mouse monoclonal anti-GFP antibody (Abmart; cat. no. M20000L; 1:100 dilution) and an equal volume of dilution buffer, respectively, for 4 h at 4°C on a rotating wheel and then mixed with 8% of volume protein-A agarose beads (25% pre-equilibrated slurry) for an additional 2 h. The beads were sequentially washed twice each with low-salt wash buffer (150 mM NaCl, 20 mM Tris-HCl [pH 8.0], 0.2% SDS, 0.5% Triton-X 100, and 2 mM EDTA), high-salt wash buffer (500 mM NaCl, 20 mM Tris-HCl [pH 8.0], 0.2% SDS, 0.5% Triton-X 100, and 2 mM EDTA), LiCl wash buffer (250 mM LiCl, 10 mM Tris-HCl [pH 8.0], 1% NP-40, 0.1% sodium deoxycholate, and 1 mM EDTA), and TE wash buffer (10 mM Tris-HCl [pH 8.0], and 1 mM EDTA). After the wash, the protein-DNA complexes were eluted from beads by adding 250 μ l of elution buffer (1% SDS and 0.1 M NaHCO₃) twice with gentle shaking for 15 min and collected by centrifugation at 3800 *g* for 2 min at room temperature. To reverse cross-linking, the sample (~500 μ l), including the pre-saved input DNA control, was treated with 20 μ l of 5 M NaCl to a final concentration of 200 mM and then incubated at 65°C for at least 4 h to overnight. After reverse cross-linking, the samples were treated with 10 μ l of 0.5 M EDTA (pH 8.0), 20 μ l of 1 M Tris-HCl (pH 6.5), and 1.5 μ l of 20 mg/ml proteinase K for 1.5 h at 45°C. The extraction of DNA was performed using the phenol-chloroform method with glycogen as a carrier for the precipitation. The resulting DNA samples were subjected to qPCR analysis using primers specific to amplicons A1–A4 (see Figure 2A and Supplemental Table 4) as described under “quantitative RT-PCR”. The enrichment fold is indicated by the ratio of ChIP DNA over input DNA.

¹⁵N uptake analysis and nitrogen use efficiency analysis

To conduct nitrogen influx measurement in roots, 2-week-old seedlings hydroponically grown under HN (1.46 mM NH₄NO₃) conditions were rinsed in 1 mM CaSO₄ solution for 1 min and then cultured in nutrient solution containing 1.46 mM ¹⁵N₂-labeled NH₄NO₃ (98 atom % ¹⁵N; Sigma; cat. no. 366528-1G) for 30 min, followed by washing in 1 mM CaSO₄ solution for 1 min. Root samples were ground into a fine powder in liquid nitrogen, and approximately 0.3–0.5 mg of each sample was collected for ¹⁵N determination using an isotope ratio mass spectrometer with an elemental analyzer (Thermo Finnigan Delta^{plus} XP; Flash EA 1112). Plant NUE was determined by the ratio of actual grain yield to applied fertilized nitrogen per plant.

Determination of Fd-GOGAT activity

Analysis of Fd-GOGAT enzyme activity was performed as described previously (Wang et al., 2018a). Briefly, plant extracts were prepared by grinding ~2 g fresh leaves of 3-week-old seedlings in 1 ml of cold extraction buffer (50 mM HEPES [pH 7.5], 15 mM KCl, 1 mM EDTA, 1 mM DTT, and 1 mM PMSF) at 4°C and then clearing by centrifugation at 20 000 *g* for 10 min at 4°C, followed by collection of the supernatants

Ghd7 enhances rice nitrogen utilization and yield

on ice. To analyze Fd-GOGAT activity, 200 μ l plant extracts (~240 μ g protein) was mixed with 800 μ l reaction mixture (50 mM HEPES [pH 8.5], 1% [v/v] β -mercaptoethanol, 3.65 mM glutamine, 3 mM α -oxoglutarate, 0.2 mM NADPH, and 0 or 4 μ M ferredoxin) and then transferred into a quartz cuvette incubated in a DU 800 nucleic acid/protein analyzer (Beckman Coulter, USA) at 37°C for the kinetics/time run. The Fd-GOGAT activity (nmol NADPH oxidized [37°C, pH 8.5]/min/mg protein) was measured spectrophotometrically by recording the rate of NADPH oxidation at 340 nm (indicated by a change in the absorbance at 340 nm blanked using reaction mixture without the addition of NADPH) and corrected by the rate measured from the reaction mixture without ferredoxin.

DATA AND CODE AVAILABILITY

Data and materials generated in this study are available without restriction upon reasonable request from the corresponding author. Source data for all figures are provided with the paper.

SUPPLEMENTAL INFORMATION

Supplemental information is available at *Molecular Plant Online*.

FUNDING

This study was supported by grants from the Ministry of Science and Technology of the People's Republic of China (2016YFD0100706), the Ministry of Agriculture and Rural Affairs of China (2016ZX08009003-004), and the State Key Laboratory of Plant Genomics (SKLPG2016A-22).

AUTHOR CONTRIBUTIONS

J. Zuo, F.C., Q.W., Q.Q., X.X., W.Q., S.L., and H.-S.G. designed the experiments and analyzed the data. Q.W. performed most experiments, with assistance of Q.S., J.N., J. Zhang, M.G., G.D., J.H., R.W., and C.W. Q.W., G.L., and W.W. performed the geographical distribution analyses. J. Zuo and Q.W. wrote the paper. All authors read and commented on the paper.

ACKNOWLEDGMENTS

We thank Drs. Yongzhong Xing and Qifa Zhang for providing the OX-*Ghd7* seeds. No competing interests declared.

Received: January 26, 2021

Revised: March 2, 2021

Accepted: April 25, 2021

Published: April 27, 2021

REFERENCES

- Chen, A., and Dubcovsky, J. (2012). Wheat TILLING mutants show that the vernalization gene *VRN1* down-regulates the flowering repressor *VRN2* in leaves but is not essential for flowering. *PLoS Genet.* **8**:e1003134.
- Deng, W., Casao, M.C., Wang, P., Sato, K., Hayes, P.M., Finnegan, E.J., and Trevaskis, B. (2015). Direct links between the vernalization response and other key traits of cereal crops. *Nat. Commun.* **6**:5882.
- Dentener, F., Drevet, J., Lamarque, J.F., Bey, I., Eickhout, B., Fiore, A.M., Hauglustaine, D., Horowitz, L.W., Krol, M., Kulshrestha, U.C., et al. (2006). Nitrogen and sulfur deposition on regional and global scales: a multimodel evaluation. *Glob. Biogeochem. Cycles* **20**:GB4003.
- Galloway, J.N., Dentener, F.J., Capone, D.G., Boyer, E.W., Howarth, R.W., Seitzinger, S.P., Asner, G.P., Cleveland, C.C., Green, P.A., Holland, E.A., et al. (2004). Nitrogen cycles: past, present, and future. *Biogeochemistry* **70**:153–226.
- Galloway, J.N., Townsend, A.R., Erisman, J.W., Bekunda, M., Cai, Z., Freney, J.R., Martinelli, L.A., Seitzinger, S.P., and Sutton, M.A. (2008). Transformation of the nitrogen cycle: recent trends, questions, and potential solutions. *Science* **320**:889–892.

Ghd7 enhances rice nitrogen utilization and yield

Molecular Plant

- Gao, Z., Wang, Y., Chen, G., Zhang, A., Yang, S., Shang, L., Wang, D., Ruan, B., Liu, C., Jiang, H., et al. (2019). The *indica* nitrate reductase gene *OsNR2* allele enhances rice yield potential and nitrogen use efficiency. *Nat. Commun.* **10**:5207.
- Good, A.G., Shrawat, A.K., and Muench, D.G. (2004). Can less yield more? Is reducing nutrient input into the environment compatible with maintaining crop production? *Trends Plant Sci.* **9**:597–605.
- Green, M.R., and Sambrook, J. (2012). *Molecular Cloning: A Laboratory Manual*, 4th edition, Vol. II (Cold Spring Harbor Laboratory Press).
- Harmer, S.L., Hogenesch, J.B., Straume, M., Chang, H.S., Han, B., Zhu, T., Wang, X., Kreps, J.A., and Kay, S.A. (2000). Orchestrated transcription of key pathways in *Arabidopsis* by the circadian clock. *Science* **290**:2110–2113.
- Hellens, R.P., Allan, A.C., Friel, E.N., Bolitho, K., Grafton, K., Templeton, M.D., Karunairetnam, S., Gleave, A.P., and Laing, W.A. (2005). Transient expression vectors for functional genomics, quantification of promoter activity and RNA silencing in plants. *Plant Methods* **1**:13.
- Higo, K., Ugawa, Y., Iwamoto, M., and Korenaga, T. (1999). Plant cis-acting regulatory DNA elements (PLACE) database: 1999. *Nucleic Acids Res.* **27**:297–300.
- Hu, B., Wang, W., Ou, S., Tang, J., Li, H., Che, R., Zhang, Z., Chai, X., Wang, H., Wang, Y., et al. (2015). Variation in *NRT1.1B* contributes to nitrate-use divergence between rice subspecies. *Nat. Genet.* **47**:834–838.
- Hudson, M.E., and Quail, P.H. (2003). Identification of promoter motifs involved in the network of phytochrome A-regulated gene expression by combined analysis of genomic sequence and microarray data. *Plant Physiol.* **133**:1605–1616.
- Jiao, Y., Ma, L., Strickland, E., and Deng, X.-W. (2005). Conservation and divergence of light-regulated genome expression patterns during seedling development in rice and *Arabidopsis*. *Plant Cell* **17**:3239–3256.
- Krapp, A. (2015). Plant nitrogen assimilation and its regulation: a complex puzzle with missing pieces. *Curr. Opin. Plant Biol.* **25**:115–122.
- Li, S., Tian, Y., Wu, K., Ye, Y., Yu, J., Zhang, J., Liu, Q., Hu, M., Li, H., Tong, Y., et al. (2018). Modulating plant growth-metabolism coordination for sustainable agriculture. *Nature* **560**:595–600.
- Liu, Y., Wang, H., Jiang, Z., Wang, W., Xu, R., Wang, Q., Zhang, Z., Li, A., Liang, Y., Ou, S., et al. (2021). Genomic basis of geographical adaptation to soil nitrogen in rice. *Nature* **590**:600–605.
- Lu, L., Yan, W., Xue, W., Shao, D., and Xing, Y. (2012). Evolution and association analysis of *Ghd7* in rice. *PLoS One* **7**:e34021.
- Ma, X., Zhang, Q., Zhu, Q., Liu, W., Chen, Y., Qiu, R., Wang, B., Yang, Z., Li, H., Lin, Y., et al. (2015). A robust CRISPR/Cas9 system for convenient, high-efficiency multiplex genome editing in monocot and dicot plants. *Mol. Plant* **8**:1274–1284.
- McAllister, C.H., Beatty, P.H., and Good, A.G. (2012). Engineering nitrogen use efficient crop plants: the current status. *Plant Biotechnol. J.* **10**:1011–1025.
- Ream, T.S., Woods, D.P., and Amasino, R.M. (2012). The molecular basis of vernalization in different plant groups. *Cold Spring Harb. Symp. Quant. Biol.* **77**:105–115.
- Saito, H., Okumoto, Y., Tsukiyama, T., Xu, C., Teraishi, M., and Tanisaka, T. (2019). Allelic differentiation at the *E1/Ghd7* locus has allowed expansion of rice cultivation area. *Plants* **8**:550.
- Saleh, A., Alvarez-Venegas, R., and Avramova, Z. (2008). An efficient chromatin immunoprecipitation (ChIP) protocol for studying histone modifications in *Arabidopsis* plants. *Nat. Protoc.* **3**:1018–1025.
- Singh, H., Verma, A., Ansari, M.W., and Shukla, A. (2014). Physiological response of rice (*Oryza sativa* L.) genotypes to elevated nitrogen applied under field conditions. *Plant Signal. Behav.* **9**:e29015.
- Ta, T.C., and Ohira, K. (1981). Effects of various environmental and medium conditions on the response of *Indica* and *Japonica* rice plants to ammonium and nitrate nitrogen. *Soil Sci. Plant Nutr.* **27**:347–355.
- Tang, W., Ye, J., Yao, X., Zhao, P., Xuan, W., Tian, Y., Zhang, Y., Xu, S., An, H., Chen, G., et al. (2019). Genome-wide associated study identifies NAC42-activated nitrate transporter conferring high nitrogen use efficiency in rice. *Nat. Commun.* **10**:5279.
- Tzfira, T., Tian, G.-W., Lacroix, B.t., Vyas, S., Li, J., Leitner-Dagan, Y., Krichevsky, A., Taylor, T., Vainstein, A., and Citovsky, V. (2005). pSAT vectors: a modular series of plasmids for autofluorescent protein tagging and expression of multiple genes in plants. *Plant Mol. Biol.* **57**:503–516.
- Wallsgrave, R.M., Turner, J.C., Hall, N.P., Kendall, A.C., and Bright, S.W.J. (1987). Barley mutants lacking chloroplast glutamine synthetase-biochemical and genetic analysis. *Plant Physiol.* **83**:155–158.
- Wang, C.-C., Yu, H., Huang, J., Wang, W.-S., Faruquee, M., Zhang, F., Zhao, X.-Q., Fu, B.-Y., Chen, K., Zhang, H.-L., et al. (2020). Towards a deeper haplotype mining of complex traits in rice with RFGB v2.0. *Plant Biotechnol. J.* **18**:14–16.
- Wang, Q., Xie, W., Xing, H., Yan, J., Meng, X., Li, X., Fu, X., Xu, J., Lian, X., Yu, S., et al. (2015). Genetic architecture of natural variation in rice chlorophyll content revealed by a genome-wide association study. *Mol. Plant* **8**:946–957.
- Wang, Q., Nian, J., Xie, X., Yu, H., Zhang, J., Bai, J., Dong, G., Hu, J., Bai, B., Chen, L., et al. (2018a). Genetic variations in *ARE1* mediate grain yield by modulating nitrogen utilization in rice. *Nat. Commun.* **9**:735.
- Wang, W., Mauleon, R., Hu, Z., Chebotarov, D., Tai, S., Wu, Z., Li, M., Zheng, T., Fuentes, R.R., Zhang, F., et al. (2018b). Genomic variation in 3,010 diverse accessions of Asian cultivated rice. *Nature* **557**:43–49.
- Wang, Y., Wang, D., Shi, P., and Omasa, K. (2014). Estimating rice chlorophyll content and leaf nitrogen concentration with a digital still color camera under natural light. *Plant Methods* **10**:36.
- Wang, Z.-Y., Kenigsbuch, D., Sun, L., Harel, E., Ong, M.S., and Tobin, E.M. (1997). A Myb-related transcription factor is involved in the phytochrome regulation of an *Arabidopsis* *Lhcb* gene. *Plant Cell* **9**:491–507.
- Weng, X., Wang, L., Wang, J., Hu, Y., Du, H., Xu, C., Xing, Y., Li, X., Xiao, J., and Zhang, Q. (2014). *Grain number, plant height, and heading date7* is a central regulator of growth, development, and stress response. *Plant Physiol.* **164**:735–747.
- Woods, D.P., McKeown, M.A., and Dong, Y. (2016). Evolution of *VRN2/Ghd7*-like genes in vernalization-mediated repression of grass flowering. *Plant Physiol.* **170**:2124–2135.
- Wu, K., Wang, S., Song, W., Zhang, J., Wang, Y., Liu, Q., Yu, J., Ye, Y., Li, S., Chen, J., et al. (2020). Enhanced sustainable green revolution yield via nitrogen-responsive chromatin modulation in rice. *Science* **367**:eaaz2046.
- Xu, G., Fan, X., and Miller, A.J. (2012). Plant nitrogen assimilation and use efficiency. *Annu. Rev. Plant Biol.* **63**:153–182.
- Xue, W., Xing, Y., Weng, X., Zhao, Y., Tang, W., Wang, L., Zhou, H., Yu, S., Xu, C., Li, X., et al. (2008). Natural variation in *Ghd7* is an important regulator of heading date and yield potential in rice. *Nat. Genet.* **40**:761–767.
- Yang, L., Liu, T., Li, B., Sui, Y., Chen, J., Shi, J., Wing, R.A., and Chen, M. (2012). Comparative sequence analysis of the *Ghd7* orthologous

Molecular Plant

regions revealed movement of Ghd7 in the grass genomes. *PLoS One* **7**:e50236.

Yang, M., Lu, K., Zhao, F.-J., Xie, W., Ramakrishna, P., Wang, G., Du, Q., Liang, L., Sun, C., Zhao, H., et al. (2018). Genome-wide association studies reveal the genetic basis of ionic variation in rice. *Plant Cell* **30**:2720–2740.

Yang, X., Nian, J., Xie, Q., Feng, J., Zhang, F., Jing, H., Zhang, J., Dong, G., Liang, Y., Peng, J., et al. (2016). Rice ferredoxin-dependent glutamate synthase regulates nitrogen-carbon metabolomes and is genetically differentiated between *japonica* and *indica* subspecies. *Mol. Plant* **9**:1520–1534.

Ghd7 enhances rice nitrogen utilization and yield

Ye, T., Li, Y., Zhang, J., Hou, W., Zhou, W., Lu, J., Xing, Y., and Li, X. (2019). Nitrogen, phosphorus, and potassium fertilization affects the flowering time of rice (*Oryza sativa* L.). *Glob. Ecol. Conserv.* **20**:e00753.

Zhang, S., Zhang, Y., Li, K., Yan, M., Zhang, J., Yu, M., Tang, S., Wang, L., Qu, H., Luo, L., et al. (2021). Nitrogen mediates flowering time and nitrogen use efficiency via floral regulators in rice. *Curr. Biol.* **31**:671–683.

Zheng, T., Yu, H., Zhang, H., Wu, Z., Wang, W., Tai, S., Chi, L., Ruan, J., Wei, C., Shi, J., et al. (2015). Rice functional genomics and breeding database (RFGB): 3K-rice SNP and InDel sub-database. *Chin. Sci. Bull.* **60**:367–371.